Available online at www.sciencedirect.com
ScienceDirect
Nuclear Instruments and Methods in Physics Research A 571 (2007) 98–101
NUCLEAR INSTRUMENTS & METHODS IN PHYSICS RESEARCH Section A
www.elsevier.com/locate/nima

Performance analysis of a low-cost small animal PET/SPECT scanner

Pedro Guerra*, Jose L. Rubio, Juan E. Ortuño, Georgios Kontaxakis, Maria J. Ledesma, Andres Santos

B104 ETS de Telecomuniación, Universidad Politécnica de Madrid, 28040 Madrid, Spain

Available online 3 November 2006

Abstract

In this work the performance of novel small animal positron/single-photon emission (PET/SPECT) scanner is estimated via Monte Carlo simulation, considering a YAP/LSO phoswich detector. To overcome the differences between PET and SPECT and in order to simplify the design, the system implements most signal processing digitally with programmable devices. The estimated performance of the described setup, expressed in terms of spatial image resolution and sensitivity, is 1.4 mm/0.6% for PET and 2.5 mm/0.025% for SPECT, figures that are comparable with state of the art dedicated scanners.

PACS: 87.62.+n; 87.53.Wz; 87.58.Ce; 87.58.Fg; 24.10.Lx

Keywords: Monte Carlo simulation; Small animal PET; Small animal SPECT

1. Introduction

PET and SPECT are fundamental techniques for the non-invasive monitorization of chemical pathways in living subjects [1] and are regarded as powerful tools for the research with animal models of human diseases, which enable not only assessing the disease progression but investigating the response to therapy as well. However, imaging small rodents is particularly challenging due to the resolution and sensitivity requirements for visualizing the functions of the animal organs [1,2]. These requirements are not met by commercial human scanners and have motivated the design of dedicated small animal scanners by research groups worldwide.

Currently there is a growing interest in simultaneously tracing various related biological processes, which is much more problematic with PET than with SPECT, because SPECT tracers may have different energy levels, while PET quanta are emitted at a fixed energy [3]. As a result, both emission techniques are not mutually exclusive and it has even been shown that in some particular situations, simultaneous acquisitions may have advantages over separate acquisitions [4]. These facts have motivated several authors to design combined PET/SPECT systems [5–8].

In this context, our goal is to specify a flexible low-cost PET/SPECT system, whose performance must be comparable in terms of sensitivity, count rate and spatial and energy resolutions with existing state-of-the art single-modality devices. The aim of this work is to assess via simulation at system level the expected performance of a scanner based on an acquisition front-end currently under development, considering a YAP/LSO phoswich.

2. Material and methods

2.1. Software tools

The performance of the proposed scanner has been estimated with the Geant4 Application for Tomographic Emission (GATE) v2.2.0 [9]. This software package, which is specific to tomographic emission, encapsulates the Geant4 libraries to achieve a modular and versatile toolkit adapted to the field of nuclear medicine. In order to accurately characterize the phoswich detector we have considered DETECT2000 [10] to estimate the overall quantum efficiency for each layer of the detector phoswich.

*Corresponding author. Tel.: +34 913367366; fax: +34 91 3367323.
E-mail address: pguerra@die.upm.es (P. Guerra).

0168-9002/$ - see front matter © 2006 Elsevier B.V. All rights reserved.
doi:10.1016/j.nima.2006.10.038

The acquisition electronics have been parameterized based on simulations obtained with the system model presented in Ref. [11]. The simulated list mode output has been reconstructed with the Open Source software package for tomographic imaging reconstruction STIR 1.4 [12] and with the sparse iterative reconstruction library ASPIRE^{TM} [13].

2.2. Design concept

The proposed scanner consists of a rotating gantry that mounts four detector blocks, each of which integrates all the detection and processing electronics. These electronics, as described in Ref. [14], consist on a H8500 photomultiplier [15], an analog interface, a set of ADCs sampling at a fixed frequency and a FPGA that performs digital pulse processing and data streaming. Moreover the detectors include detachable parallel-hole collimators in order to enable different configurations, i.e., PET-only, SPECT-only and combined PET/SPECT.

In the design of the detector, the scintillation material plays a significant role. The proposed scanner assumes a phoswich detector with two layers of 25×25 pixellated crystals of $15 \times 2 \times 2$ mm each. The front layer is based on cerium-activated yttrium aluminum perovskite (YAP), whose time resolution is comparable to other fast scintillators. Although its excellent spectroscopic and timing properties are limited by a low photofraction at 511 keV [16]. The back layer is based on lutetium oxyorthosilicate (LSO) [17], which is nowadays the crystal of choice for PET due to its excellent physical properties. This layer setup is motivated by the intrinsic radioactivity of the LSO originating from the ^{176}Lu, which produces a background count rate around 5–20 cps/crystal that raises some concerns in using LSO in SPECT. This way, low energy SPECT photons will be mostly detected in the YAP layer, while PET quanta detections will be evenly distributed between both layers.

2.3. Simulation setup

GATE has been used to describe a four-detector heads scanner with 18 cm of diameter, as shown in Fig. 1. In the simulated scenario, a 20 mm lead collimator, with 0.6 mm hole-diameter and a 0.15 mm gap between the hexagonally arranged holes, is placed on top of two opposite detectors, while the other pair is left uncovered. For a proper description of the phoswich, parameters such as light yield, intrinsic resolution and transfer efficiency are specified based on results from DETECT2000. Additionally, other parameters of the different elements of the front-end are specified according to previous studies: time resolution is set to 2 ns, the time window to 10 ns and dead time is set as paralyzable/non-paralyzable 260 ns for acquisition, and non-paralyzable 800 ns for the transmission of the acquired data. With these settings, we have estimated the performance for the worst-case scenario: two heads in coincidence mode for PET and two heads in single mode for SPECT.

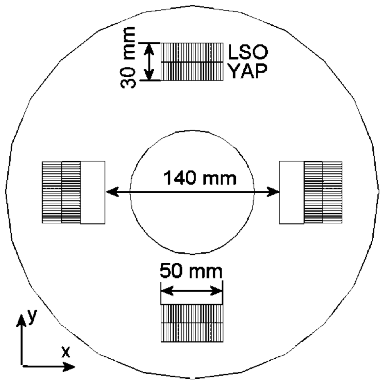

Fig. 1. Diagram of the simulated scanner, consisting of four identical rotating heads, two of which mount a parallel-hole lead collimator.

3. Results

3.1. Scanner performance in PET mode

Resolution in PET mode has been computed as the FWHM of a box around the peak of the reconstructed volume, using the 3D-FBP provided by STIR. Additional simulations where carried out in order to compute the scanner's noise-equivalent count (NEC) curve for the pair of detectors in PET mode. For this purpose we simulated a 2 cm radius and 5 cm height cylinder placed in the center of the field of view (FOV), filled with water and with a uniform activity distribution.

Fig. 2 shows the estimated spatial resolution in PET mode for five point sources distributed along the radial axis with different layer identification error rates, showing that the ability of the electronics to identify the crystal of interaction guarantees very low resolution degradation due to depth of interaction (DOI), even when the crystal classification error goes as high as 10%. Resolution remains almost constant in the full FOV, enabling the visualization of small activity points in the edge of the FOV, as shown in the reconstructed Derenzo phantom of Fig. 2.

The estimated performance in PET mode is comparable in terms of resolution and sensitivity with state of the art PET scanners, as it is shown in Table 1. This table considers two PET scanners: the YAPPET [7], from the University of Ferrara, and the Micropet FOCUS [18], from CTI Molecular Imaging.

Results show that, thanks to the phoswich approach, the expected resolution is homogeneous within the FOV. However the sensitivity is 6 times lower than in the FOCUS scanner, due to the smaller solid angle covered with only two detectors, although it is still comparable to the YAPPET, if we account for the fact that in Ref. [7] sensitivity is computed with four heads and with a wide-energy window.

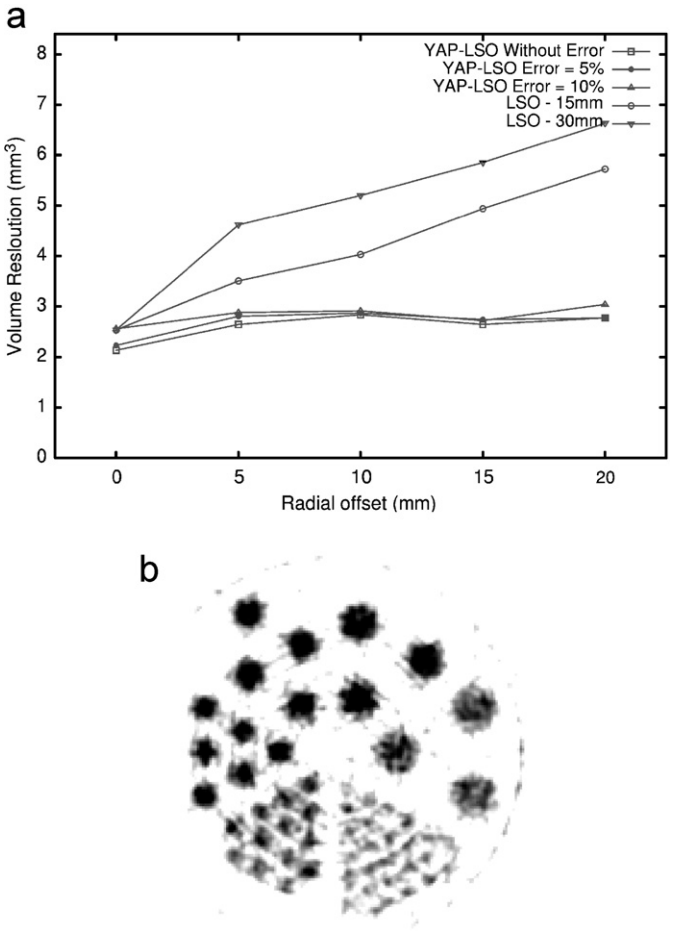

Fig. 2. (a) Estimated radial resolution of the phoswich for five point sources in PET mode, with a 0%, 5% and 10% crystal identification error. As reference, resolution is also computed with a LSO-only detector with crystals 15 and 30 mm long. (b) PET phantom reconstructed with the STIR's FBP-3D and $3.5e^6$ counts, consisting of 0.6 mm (bottom right), 0.8, 1.2, 1.6, 2.0 and 2.4 mm bars (clockwise).

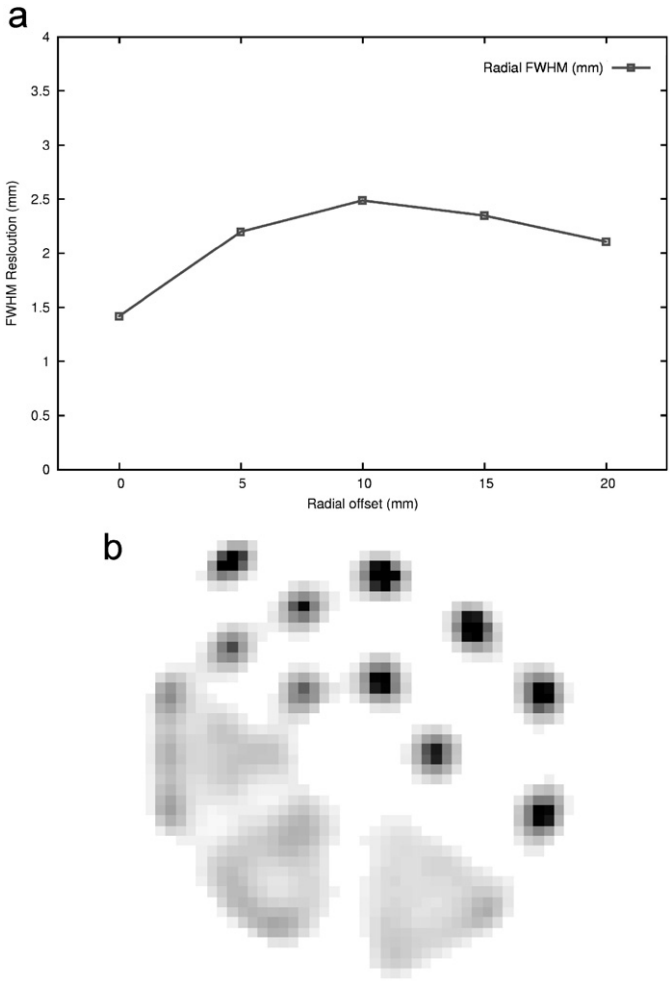

Fig. 3. (a) Estimated radial resolution in SPECT at 140 keV mode for five point sources at 0, 5, 10, 15 and 20 mm from the FOV center with the described collimator. (b) Reconstructed image in SPECT mode at 140 keV with ASPIRE's OSEM implementation and $2.3e^6$ counts.

Table 1
Scanners performance: state-of-the-art vs simulation results

		PET at 511 keV	SPECT at 140 keV
microPET Focus [18]	Sensitivity	3.4%	—
	Resolution	1.3 mm	
X-SPECT [19]	Sensitivity	—	0.014%
	Resolution		2.2 mm
YAPPET [7]	Sensitivity	1.7%	0.01%
	Resolution	1.8 mm	3.5 mm
YAP/LSO Simulations	Sensitivity	0.6%	0.025%
	Resolution	<1.4 mm	<2.5 mm

3.2. Scanner performance in SPECT mode

Regarding acquisition in SPECT mode, Fig. 3 shows the estimated resolution along the radial axis after reconstruction with the ASPIRE^{TM} software package. In this case, the worst radial resolution is located halfway between the center and border of the FOV. The reconstructed Derenzo phantom confirms the capability of the proposed scanner to distinguish lesions down to 2 mm.

The estimated performance in SPECT mode is comparable in terms of resolution and sensitivity to state of the art SPECT scanners, as it is shown in Table 1. This table considers again two scanners: the YAPPET from the University of Ferrara and the X-SPECT [19] from Gamma Medica-IDEAS. Compared to the hybrid YAPPET scanner, the proposed architecture would provide higher sensitivity and resolution due to the higher area of the individual detector, being the actual figures close to those of the X-SPECT, although comparison is not straightforward, due to differences in the collimator.

4. Conclusions

The performance of a novel PET/SPECT scanner for small animals has been estimated via simulation, considering a YAP/LSO phoswich detector. Simulation results have

shown the feasibility of the proposed detector for a hybrid SPECT/PET scanner, being the estimated performance very close to best-in-class dedicated scanners. In PET mode, the estimated sensitivity meets the expectations for 2-head detectors while resolution remains almost constant for the whole FOV, thanks to the phoswich approach. Moreover, results show that resolution degradation due to crystal misidentification is not severe as far as the error rate is kept below 10%. Regarding SPECT, the resulting spatial resolution and reconstructed image are satisfactory. However no proper optimization has been carried out regarding the collimator, therefore additional resolution improvements may still be achieved. Finally Derenzo-like phantoms have been simulated and reconstructed in both modalities, showing that with the proposed configuration it is possible to visualize small structures, despite the reduced number of detectors.

As future work, we plan to tune system parameters for SPECT imaging with low energy isotopes and analyze potential performance degradation and reconstruction corrections with simultaneous PET/SPECT acquisitions.

Acknowledgments

This work has been supported by FPU Program of the Spanish Education and Science Ministry, by the EU-funded EMIL network (LSHC-CT-2004-503569), the joint Research Action HG04-6 and the research projects TEC2004-07052-C02 and IM3 (PI052204). Finally we thank Prof. Fessler and the University of Michigan for providing the ASPIRE software.

References

[1] R. Lecomte, Nucl. Inst. & Meth. A 527 (2004) 157.
[2] M. Kapusta, et al., IEEE Trans. Nucl. Sci. 47 (2000) 1341.
[3] T.C. Rust, et al., Phys. Med. Biol. 51 (2006) 61.
[4] E. Di-Bella, et al., J. Nucl. Med. 42 (2001) 944.
[5] M. Dahlbom, et al., IEEE Trans. Nucl. Sci. NS44 (1997) 1114.
[6] A. Saoudi, et al., IEEE Trans. Nucl. Sci. NS46 (1999) 479.
[7] A. Del Guerra, et al., IEEE Trans. Nucl. Sci. NS47 (2000) 1537.
[8] B.J. Pichler, et al., IEEE Trans. Nucl. Sci. NS50 (2003) 1420.
[9] S. Jan, et al., Phys. Med. Biol. 49 (2004) 4543.
[10] F. Cayouette, et al., IEEE Trans. Nucl. Sci. NS50 (2003) 339.
[11] P. Guerra, et al., IEEE Nucl. Sci. Symp. 5 (2004) 3089.
[12] K. Thielemans, et al. Software for Tomographic Image Reconstruction, 2004 (online).
[13] J.A. Fessler, ASPIRE 3.0 User's Guide A Sparse Iterative Reconstruction Library, 1995.
[14] P. Guerra, et al. IEEE Trans. Nucl. Sci. NS53 (2006) 770.
[15] Hamamatsu, H8500 Datasheet, 2003.
[16] M. Moszynski, et al., Nucl. Inst. & Meth. A 404 (1998) 157.
[17] C.L. Melcher, et al., IEEE Trans. Nucl. Sci. NS39 (1992) 502.
[18] Y.-C. Tai, et al., 46 (2005) 455.
[19] Gamma Medica Inc., website (2001).